JOURNAL OF SOLID STATE CHEMISTRY 58, 78–86 (1985)

Crystal Structure Relationships in the System $SnS–Sb_2S_3$

P. P. K. SMITH

Research School of Chemistry, Australian National University, GPO Box 4, Canberra, ACT 2601, Australia

Received July 12, 1984; in revised form October 22, 1984

The crystal structures of Sb_2S_3 and the five ternary compounds of composition $m:n$ = 3:1, 2:1, 4:3, 6:5, and 1:1 on the join $(SnS)_m$–$(Sb_2S_3)_n$ are built from ribbons of edge-sharing MS_5 pyramids; SnS contains the same substructure in the form of infinite two-dimensional sheets. The ribbons lie in two orientations 50–58° apart and are either independent, or linked by shared sulfur atoms. The metal atoms lie in trigonal prismatic sites created by the juxtaposition of the ribbons; the prisms are capped by a single pyramid, except for metal sites which lie in the acute angle between two hinged ribbons—in such cases the prism is bicapped. The underlying structure-building principle involves the elimination of cation sites from the SnS structure in order to accommodate the stoichiometry of the Sb_2S_3 component, while maintaining approximately uniform coordination for the metal sites across the series.

Introduction

The ternary system Sn–Sb–S has been the subject of a number of phase equilibrium studies leading to somewhat contradictory results, particularly with regard to phase relations on the join $SnS–Sb_2S_3$. Research on this system prior to 1975 has been reviewed comprehensively by Moh (*1*) and will not be considered in detail here. A significant contribution to our understanding of this system was made by Wang and Eppelsheimer (*2*), who reported unit cell parameters for phases of composition 3:1, 2:1, and 1:1, where $m:n$ denotes the ratio of the end-member components $SnS:Sb_2S_3$. Subsequent studies have confirmed the existence of the 3:1 and 2:1 phases (*3*, *4*), but a crystal structure analysis of the (monoclinic) "1:1" phase shows that its correct composition is given by the ratio 6:5 (*5*). Jumas *et al.* (*6*) synthesized a fourth compound, of composition 4:3. Finally, a 1:1 phase with orthorhombic symmetry has recently been reported by Smith and Parise (*7*), making a total of 5 known ternary compounds on the join $SnS–Sb_2S_3$.

Crystal structure analysis of these sulfosalt compounds has been hampered by the difficulty of growing single crystals of suitable quality for X-ray diffractometry, although the 6:5 and 4:3 structures were solved by this method (*5*, *6*). The 3:1 and 1:1 structures were solved by high-resolution electron microscopy (*3*, *7*); the former was subsequently refined by neutron powder diffraction (*8*) and in the case of the 1:1 composition a single-crystal X-ray refinement has been carried out on the selenium analog $SnSb_2Se_4$ (*7*). The structure of the 2:1 compound $Sn_2Sb_2S_5$ was determined by noticing the relationship of its unit cell parameters to those of stibnite and meneghinite (*4*); a single crystal X-ray re-

0022-4596/85 $3.00

TABLE I

COMPOSITIONS AND UNIT CELL DATA FOR COMPOUNDS IN THE SYSTEM $SnS-Sb_2S_3$[a]

	$m:n$	Space group	a	b	c	β	Reference
β-SnS (>878 K)	1:0	*Bbmm*[b]	11.480	4.177	4.148		(*10*)
α-SnS (<878 K)	1:0	*Pnma*[b]	11.200	3.987	4.334		(*11*)
$Sn_3Sb_2S_6$	3:1	*Pnma*	23.18	3.965	34.94		(*3, 8*)
$Sn_2Sb_2S_5$	2:1	*Pnma*	19.59	3.938	11.426		(*4*)
$Sn_4Sb_6S_{13}$	4:3	I2/*m*	24.31	3.915	23.49	94.05°	(*6*)
$Sn_6Sb_{10}S_{21}$	6:5	C2/*m*	44.995	3.9023	20.613	96.21°	(*5*)
$SnSb_2S_4$	1:1	*Pnmn*[b]	25.641	3.8973	20.381		(*7*)
Sb_2S_3	0:1	*Pnma*	11.3107	3.8363	11.2285		(*12*)

[a] The ratio $m:n$ is the mole ratio of the end member components.

[b] Space group given here in different setting from that in the original reference.

finement has also been carried out for the Bi-substituted analog $Bi_xSb_{2-x}Sn_2S_5$ (*9*).

The purpose of the present paper is to compile the structural information for the end members and the 5 ternary compounds on the join $SnS-Sb_2S_3$. A unified description is presented for these structures, which prove to be closely related.

Crystal Structures

Space group and unit cell data for the compounds under consideration are given in Table I. In all cases there is one unit cell repeat of ~4 Å perpendicular to a mirror plane and this direction is taken as the *b* crystallographic axis; the structures can then be drawn conveniently in [010] projection. Since the X-ray scattering factors for tin and antimony differ by only 2% these atomic species have not been distinguished in the structure determinations of the ternary compounds, except in the case of $Sn_4Sb_6S_{13}$ where a distinction was made on the basis of the thermal parameters for the metal sites (*6*). It should be noted that in the single crystal refinements of $Sn_6Sb_{10}S_{21}$ (*5*) and $SnSb_2Se_4$ (*7*) the fit between the calculated and observed structure factors was not significantly improved by any ordered arrangement of Sn and Sb over the available metal sites, as compared to the disordered model.

The crystal structures of the end members SnS and Sb_2S_3 are described first as these illustrate the underlying structure-building principle for the series. The ternary compounds are then considered, in order of increasing Sb content. Except where indicated otherwise, structural information is from the references listed in Table I.

β-Sns. Above 878 K SnS adopts the thallium iodide (*B*33) structure type shown in Fig. 1. The structure consists of infinite sheets of edge-sharing pyramids, with the

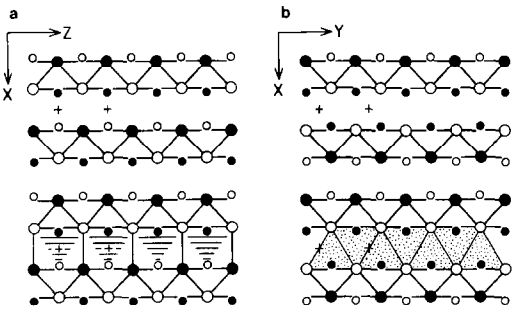

FIG. 1. The structure of β-SnS projected on (010) (a) and (001) (b). The monocapped trigonal prismatic coordination of tin is represented by line shading (horizontal prisms) or dot shading (prisms viewed end on). Small circles = Sn, large circles = S; open circles height = 0.25, filled circles height = 0.75. Crosses denote the corners of the unit cell.

metal atoms lying on the axis of the pyramid, just outside the pyramid base. Two longer bonds to sulfur atoms in the next pyramidal sheet complete the sevenfold coordination polyhedron, which is a monocapped trigonal prism as shown in the lower part of Figs. 1a and b. The metal–sulfur distances at 905 K (β-SnS cannot be quenched to room temperature) are 2.63, 4 × 2.96, and 2 × 3.74 Å, the shortest distance being that to the capping sulfur. The two long M–S distances of the trigonal prism result from the volume occupied by the lone $5s^2$ pair of electrons on the Sn^{2+} ion. The $B33$ structure can be derived from the $B1$ (NaCl) structure simply by displacing alternate layers of half-octahedra by $a/2$ along the a axis.

α-SnS. The room temperature form of SnS has the $B16$ (GeS) structure type (Fig. 2) which is closely related to $B33$. In the α form the tin atoms are displaced from the axis of the pyramid and the pyramid base departs further from an exact square, as evidenced by the b and c cell parameters for the two polymorphs. The pyramidal layers are also displaced slightly with respect to each other, causing a slight shear of the trigonal prisms. As a result of the offset of the metal atom there are three short M–S distances, the bond lengths being 2.627 (cap) and 2 × 2.665 Å (basal edge of pyramid). The four longer M–S distances are 2 × 3.290, 3.388, and 4.093 Å.

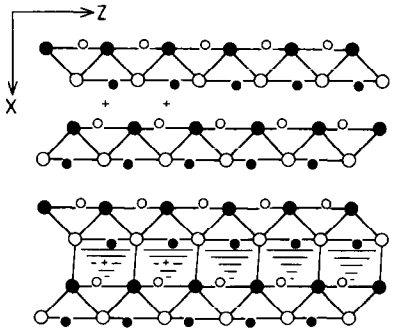

FIG. 2. The room temperature α form of SnS projected on (010). Small circles = Sn, large circles = S; open circles y = 0.25, filled circles y = 0.75. The tin atoms lie in slightly sheared trigonal prisms (line shaded) with single caps formed by the pyramidal sheets.

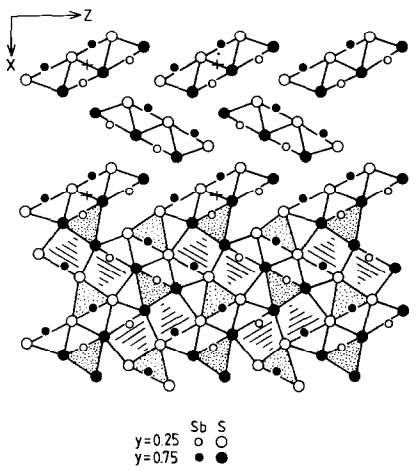

FIG. 3. The structure of stibnite Sb_2S_3 projected on (010).

The pyramidal sheet of the α-SnS structure is the basic building unit for all the compounds on the SnS–Sb_2S_3 join, but in the antimony-bearing members it occurs as ribbons of various widths extending along b, rather than as infinite two-dimensional sheets. Also, these ribbons always occur in two orientations rather than in parallel layers as in SnS itself. In all cases the metal atoms lie in trigonal prisms formed by the juxtaposition of adjacent pyramidal sheets, with one or two pyramidal caps formed by the sheets themselves.

Sb_2S_3. The upper part of Fig. 3 shows the structure of Sb_2S_3 depicted as isolated bands of the SnS structure, each band having the composition $(M_4S_6)_n$. The ribbons extend parallel to the b axis and they are related by glide reflection planes in (100) and (001). The angle between the ribbons is such that the triangular faces of the pyramids at the edge of one ribbon are approximately parallel to the basal faces of the pyramids in the adjacent ribbon; this relationship also holds for the five ternary

compounds in the system. The lower part of Fig. 3 shows that this arrangement of the ribbons gives rise to monocapped trigonal prismatic coordination for both of the two independent Sb atoms; one prism has its axis parallel to the *b* axis (dot shaded) and the other is parallel to the (010) plane (line shaded). In both cases the two longest Sb–S bonds are those to sulfur atoms in neighboring ribbons. As in the case of SnS the long metal–sulfur distances result from the stereochemical activity of the lone $5s^2$ pair of electrons, the Sb^{3+} ion being isoelectronic with Sn^{2+}.

The structure of Sb_2S_3 can thus be viewed as a simple way of achieving trigonal prismatic coordination for the metal atoms in a compound of M_2S_3 rather than MS stoichiometry. Cations are eliminated from the infinite SnS-type sheets by cutting the sheets into narrow ribbons. The pyramid coordination is thus retained and the two longest bonds of the trigonal prism are obtained by a suitable packing of ribbons in the (010) plane. This will be seen to be the case for all the phases on the $SnS-Sb_2S_3$ join, with the ribbons becoming progressively narrower as the Sb content increases, i.e., with increasing cation elimination.

$Sn_3Sb_2S_6$. The structure of $Sn_3Sb_2S_6$ (Fig. 4) consists of lozenge-shaped blocks, each block being made up of three ribbons of composition $(M_{10}S_{12})_n$. Two such lozenges comprise the unit cell, which thus has the cell contents $M_{60}S_{72}$. The ribbons of adjacent layers meet at an angle of 52° in the manner described above for Sb_2S_3. The structure within each block is close to that of β-SnS (cf. Fig. 1b), although the metal atoms are offset from the axes of the pyramids as in α-SnS. At the interface between adjacent blocks the structure solves the problem of matching the ribbon edges (triangular faces of the pyramids) to the ribbon faces (pyramid bases) by forming two "horizontal" prisms and three "upright" prisms.

All the metal atoms lie in monocapped trigonal prisms, with the exception of $M(13)$ which is in a bicapped prism. This situation arises because $M(13)$ can be considered to belong to two different ribbons, the ribbons being hinged together at this point. The

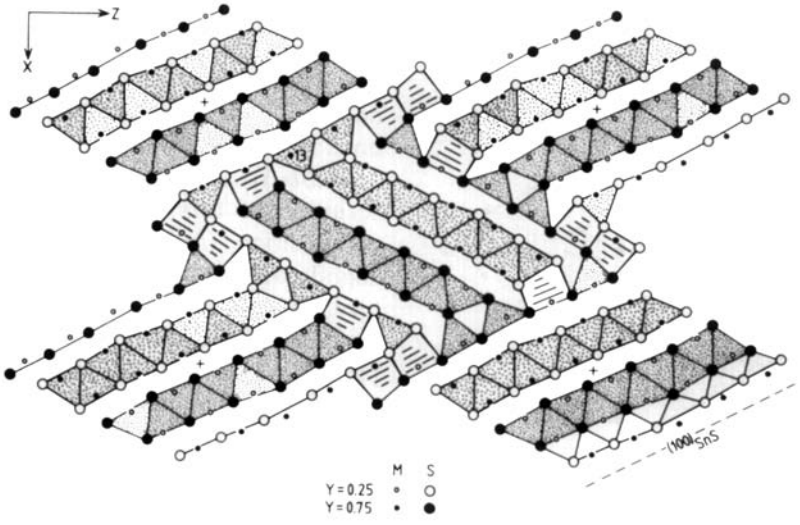

FIG. 4. The structure of $Sn_3Sb_2S_6$ projected on (010). Metal atom $M(13)$ is shared between two pyramidal ribbons and thus lies in a bicapped trigonal prism of sulfur atoms. The (100) plane of the SnS-type substructure is indicated at the bottom right.

metal atom lies in the acute angle between the two hinged ribbons and its prism is thus capped by pyramids from both ribbons. This type of coordination will also be encountered in the 4:3, 6:5, and 1:1 phases and will be described further under those headings. The articulated ribbons are readily recognized by the fact that the metal atom concerned is displaced toward the center of the prism, so as to lie approximately midway between the two caps.

$Sn_2Sb_2S_5$. The structure of the 2:1 compound (Fig. 5) is closely related to those of meneghinite and stibnite (*4*). The structure is obtained from that of Sb_2S_3 simply by doubling the width of each ribbon, to give the composition $(M_8S_{10})_n$ as required by the stoichiometry of the compound. The metal atoms close to the (100) *n*-glide planes lie in "upright" monocapped trigonal prisms, the others in horizontal prisms.

In theory this structure type is infinitely adaptive, forming compounds of stoichiometry $(MS)_n(M_2S_3)$ with ribbons $(n + 2)$ cations wide. In practice the 3:1, 2:1, and 0:1 members occur in the PbS–Sb_2S_3 system, but in the case of SnS–Sb_2S_3 the 3:1 compound $Sn_3Sb_2S_6$ is represented by the block structure described above. In these two systems the stoichiometry of Sb_2S_3 restricts the minimum ribbon width to two cations, i.e., ribbons $(M_4S_6)_n$ as in stibnite itself. It is of interest to note here that the stoichiometry SbX_2 can be attained by substituting a monovalent ion for half of the sulfur, as in the compound SbSI. Figure 6 shows that the structure of SbSI is closely related to that of stibnite, with the same space group *Pnma*, but the stoichiometry now calls for the narrowest possible ribbons $(M_2X_4)_n$.

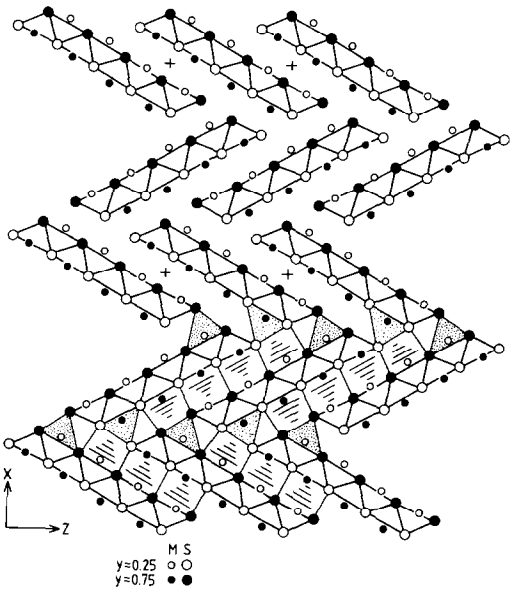

FIG. 5. The structure of $Sn_2Sb_2S_5$ projected on (010). Compare with Sb_2S_3 (Fig. 3); both structures may be derived from the SnS structure type by glide-reflection twinning on the unit cell scale.

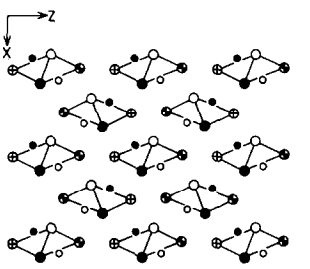

FIG. 6. The structure of the paraelectric form of SbSI projected on (010), space group *Pnma* (*21*). The ferroelectric form differs only in the heights of the atoms, which are displaced slightly from the mirror planes. Small circles = Sb, large circles = S, crosses = I. Empty symbols $y = 0.25$, filled symbols $y = 0.75$.

$Sn_4Sb_6S_{13}$. Jumas *et al.* (*6*) based their description of this structure on ribbons of composition $(M_5S_7)_n$. Figure 7 shows a slightly different interpretation of the structure, based on hinged ribbons. The structural motif consists of a wide band of composition $(M_{12}S_{14})_n$, with two ribbons $(M_5S_7)_n$ attached to it at an angle of ~50°. The narrow ribbons thus share a line of sulfur atoms with the wide ribbon at the hinge point, and metal atom *M*(6) has the double-capped prismatic coordination polyhedron characteristic of this situation. This distinctive and larger cation site accounts for the ele-

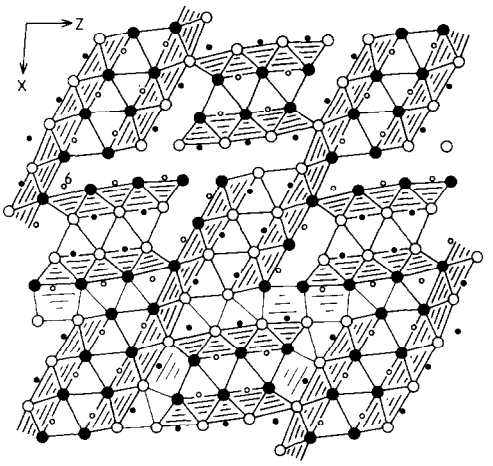

FIG. 7. The monoclinic structure of $Sn_4Sb_6S_{13}$ projected on (010). Metal atom $M(6)$ is shared between the $(M_{12}S_{14})_n$ and $(M_5S_7)_n$ ribbons.

vated thermal parameter reported for $M(6)$.

It has apparently not been noticed previously that this compound is isostructural with the mineral robinsonite $(PbS)_4(Sb_2S_3)_3$, the structure having been solved independently for the tin- and lead-bearing phases. The relationship is obscured by the fact that Petrova *et al.* (*13*) solved and refined the structure of $Pb_4Sb_6S_{13}$ in the triclinic space group $P1$, whereas the observations made by Wang (*14*) indicate that robinsonite in fact has monoclinic symmetry with a unit cell almost identical to that of $Sn_4Sb_6S_{13}$.

$Sn_6Sb_{10}S_{21}$. The upper part of Fig. 8 shows the structure of the 6:5 phase depicted as isolated ribbons of the SnS structure; the lower part of the figure shows how this leads to capped trigonal prisms of sulfur atoms about the cations. The repeat unit consists of two diad-related ribbons of composition $(M_{10}S_{12})_n$, two of composition $(M_4S_6)_n$, also diad-related, and an independent $(M_4S_6)_n$ ribbon that lies on a screw diad axis. The structure is described in more detail by Parise and Smith (*5*). Although the

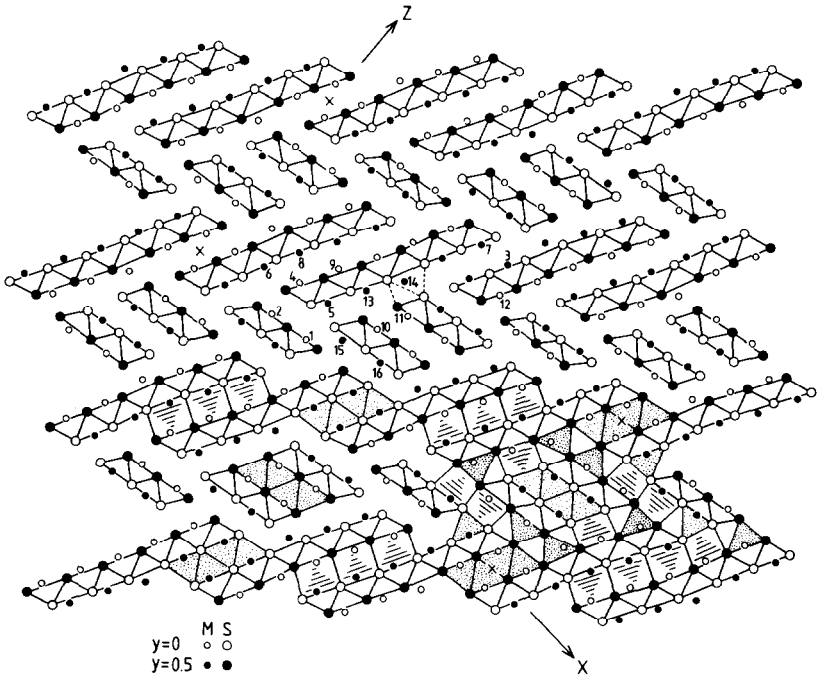

FIG. 8. (010) projection of the monoclinic structure of $Sn_6Sb_{10}S_{21}$. In the upper part of the figure the structure is depicted as isolated ribbons; notice that $M(14)$ is shared between two ribbons and has bicapped trigonal prismatic coordination. The cation numbering follows Parise and Smith (*5*).

ribbons are shown as isolated it is clear from the structure drawing that $M(14)$ is a "hinge cation," linking an $(M_{10}S_{12})$ band to an (M_4S_6) band. $M(14)$ thus has the double capped trigonal prismatic coordination characteristic of such sites, as noted already for the 3:1 and 4:3 phases. $M(14)$ has the largest thermal parameter of all the metal sites, with the thermal ellipsoid elongated towards the two caps.

$SnSb_2S_4$ and $SnSb_2Se_4$. This structure was solved by locating the metal positions in HRTEM images of the sulfide, but has only been refined for the selenide (Fig. 9). The structure consists of ribbons of composition $(M_5Se_7)_n$ that are hinged together at Se(10), with the metal atom $M(7)$ in the acute angle between two ribbons. As anticipated, $M(7)$ has a strongly anisotropic thermal parameter (Fig. 10). In addition to the linkage at Se(10) the ribbons are also joined at Se(6), forming a structural unit that is not found in any of the other compounds in the SnS–Sb_2S_3 system.

Discussion

The essential feature of this series of structures is the means by which cations are eliminated from the underlying SnS structure in order to accommodate the stoichiometry of the Sb_2S_3-containing phases. The required decrease in the cation/anion ratio is achieved by cutting the infinite pyramidal sheets into relatively narrow ribbons; the structures are then built by packing these ribbons in two orientations 50–58° apart. This configuration juxtaposes the broad (100) face of one SnS-type ribbon either with the (100) face of a parallel ribbon or with the narrow edge ((201) or (210)) of a ribbon in the alternative orientation. This situation is analogous to the matching of (100) and (111) faces of the $B1$ structure, a structure-building principle described by Makovicky (*15*) for the Pb–Bi sulfosalts. The (100) to (210) match is seen most clearly in the structure of $Sn_3Sb_2S_6$ (Fig. 4) where it is maintained across the face of a ribbon five pyramids in width. Here the "interblock" angle of 52° is close to the calculated angle of 54.0° for (100)–(210) for β-SnS, or 54.6° for α-SnS. The average width of the structural ribbons decreases with increasing Sb content, culminating in the $(M_4S_6)_n$ ribbons of Sb_2S_3.

This structure-building principle may be contrasted with crystallographic shear (*16*) and unit-cell twinning (*17*), which both modify the cation/anion ratio by forming

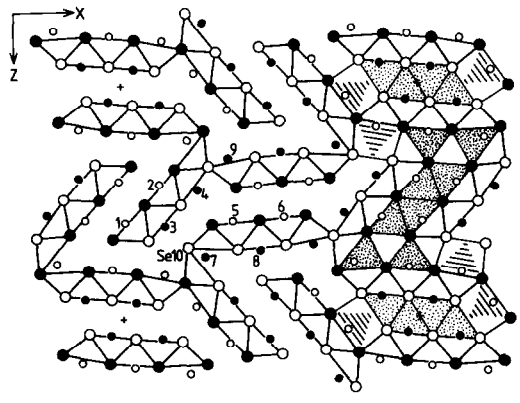

FIG. 9. Orthorhombic structure of $SnSb_2Se_4$ (and $SnSb_2S_4$) projected on (010).

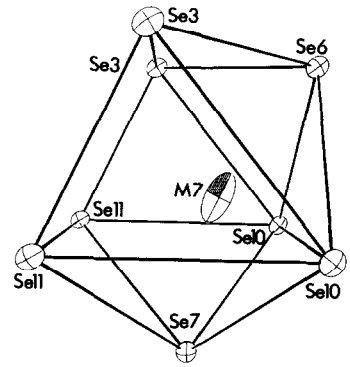

FIG. 10. The bicapped trigonal prism coordination of $M(7)$ in $SnSb_2Se_4$. Notice the large anisotropic thermal motion along a line joining the two caps. This coordination polyhedron is characteristic of metal atoms that lie in the acute angle between two hinged ribbons, as occurs in the 3:1, 4:3, 6:5, and 1:1 phases.

extended planar faults, thus generating homologous series of phases as the fault plane spacing varies. In the case of SnS–Sb_2S_3 most of the compounds are formed by faults of limited extent, and the structures depend on the existence of particular complex mosaic patterns in the (010) plane. The exception is the $Sn_2Sb_2S_5$–Sb_2S_3 homologous series (*4*) which is formed by glide reflection twinning of the SnS structure. This clearly provides a possible mechanism for accommodating nonstoichiometry (cation deficiency) in SnS, which shows considerable solid solution towards Sb_2S_3 (*1*).

Apart from the obvious structural similarities noted in the descriptions of the $(SnS)_m(Sb_2S_3)_n$ phases the structural relationship is also evidenced by a kind of Vegards law behavior in the unit cell dimensions across the series. The decrease in the *b* parameter with increasing Sb content reflects the relative size of the Sn^{2+} and Sb^{3+} ions (Table I). Thus in α-SnS the shortest metal–sulfur distance is 2.627(4) Å whereas the shortest Sb–S distance in Sb_2S_3 is 2.455(3) Å, a difference of 6.8%. Since the *a* and *c* cell parameters for the various phases cannot be compared directly it is more appropriate to consider $\sqrt[3]{V_s}$, where V_s is the unit cell volume divided by the number of sulfur atoms in the cell. In Fig. 11 this parameter is plotted against the Sn–Sb content. SnS and the five ternary compounds lie on a well-defined straight line with a difference of 6.6% between the values $\sqrt[3]{V_s}$ for the end-member compositions, in good agreement with the variation in bond lengths noted above. The small deviation of Sb_2S_3 from this line presumably results from the geometry of the particular structure—in this phase the SnS-like structural units are at their narrowest and the specific volume for sulfur thus depends critically on the efficiency of the ribbon packing. The variation in the specific volume of sulfur was used predictively by Parise and Smith (*5*) to determine the number of S atoms in the unit cell, and hence the ratio $m:n$, for $Sn_6Sb_{10}S_{21}$.

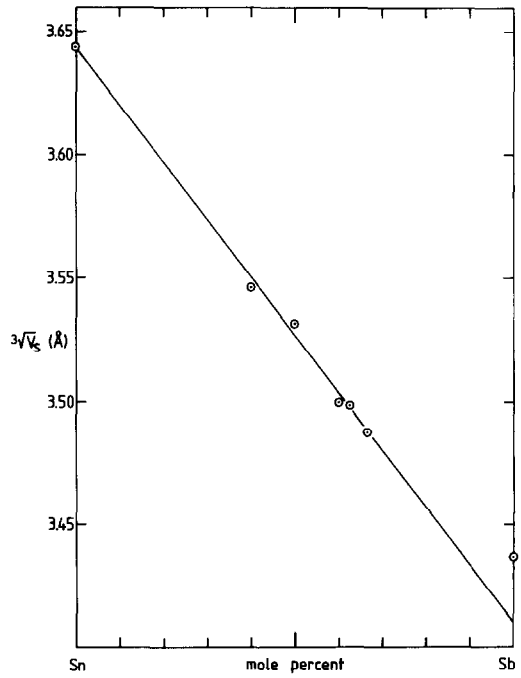

FIG. 11. Variation of $\sqrt[3]{V_s}$ with Sn–Sb content, where V_s is the unit cell volume divided by the number of sulfur atoms in the cell. The line is the least-squares best fit to the data points for SnS and the five ternary compounds.

So far we have only considered phases on the join SnS–Sb_2S_3, but it is worth briefly mentioning the closely related phases Sn_2S_3 and $Sn_5Sb_2S_9$, both of which contain Sn^{4+} in addition to Sn^{2+} (*18, 19*). Sn_2S_3 contains continuous ribbons $(M_2S_6)_n$ of the SnS_2 (= CdI_2) structure; between these ribbons the Sn^{2+} ions form narrow ribbons $(M_2S_4)_n$ of the SnS structure. $Sn_5Sb_2S_9$ bears no simple structural relationship to the other tin–antimony sulfides; Sn^{2+} is coordinated by a very distorted bicapped trigonal prism but these do not combine to form elements of the SnS structure.

Finally it should be noted that several other sulfosalt structures can be described very simply in terms of the pyramidal ribbons used to describe the SnS–Sb_2S_3

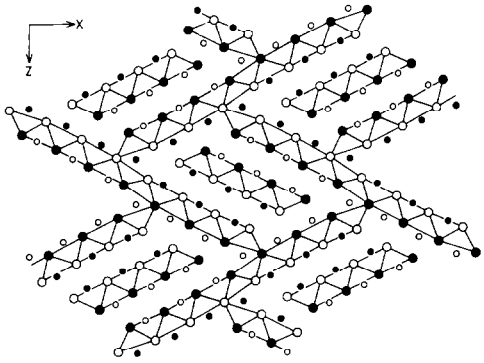

FIG. 12. Structure of boulangerite projected on (010).

phases. We have already seen that robinsonite is isostructural with $(SnS)_4(Sb_2S_3)_3$; other examples that can be considered similarly are jamesonite, boulangerite, and the synthetic phase $Pb_4Sb_4S_{11}$. These have been drawn and described by Makovicky (*15*) in terms of rods of *B*1 structure that have undergone "2 Å shear"; this is of course the same shear that transforms *B*1 to the *B*33 structure. As an example Fig. 12 shows how boulangerite $Pb_5Sb_4S_{11}$ (*20*) may be represented very simply by the linkage of $(M_{14}S_{16})_n$ strips to form a tunnel which contains a narrower $(M_6S_8)_n$ strip. As one might expect, the large cation site in the acute angle between the hinged ribbons contains Pb; consequently this site does not have the elevated thermal parameter noted for the Sn, Sb sulfosalts where a large ion is not available to fill this site.

Acknowledgments

I thank Professor B. G. Hyde for many helpful discussions, and also Professor J. S. Anderson and Dr. J. B. Parise for reviewing the manuscript. Atom positions for the structure drawings were plotted by means of the programs UNIT/PROJN written by Dr. G. R. Anstis.

References

1. G. H. MOH, *Chem. Erde* **34,** 201 (1975).
2. N. WANG AND D. EPPELSHEIMER, *Chem. Erde* **35,** 179 (1976).
3. P. P. K. SMITH, *Acta Crystallogr. C* **40,** 581 (1984).
4. P. P. K. SMITH AND B. G. HYDE, *Acta Crystallogr. C* **39,** 1498 (1983).
5. J. B. PARISE AND P. P. K. SMITH, *Acta Crystallogr.*, in press.
6. J. C. JUMAS, J. OLIVIER-FOURCADE, E. PHILIPPOT, AND M. MAURIN, *Acta Crystallogr. B* **36,** 2940 (1980).
7. P. P. K. SMITH AND J. B. PARISE, *Acta Crystallogr.*, in press.
8. J. B. PARISE, P. P. K. SMITH, AND C. J. HOWARD, *Mater. Res. Bull.* **19,** 503 (1984).
9. V. KUPCIK AND M. WENDSCHUH, *Acta Crystallogr. B* **38,** 3070 (1982).
10. H. G. VON SCHNERING AND H. WIEDEMEIER, *Z. Kristallogr.* **156,** 143 (1981).
11. H. WIEDEMEIER AND H. G. VON SCHNERING, *Z. Kristallogr.* **148,** 295 (1978).
12. P. BAYLISS AND W. NOWACKI, *Z. Kristallogr.* **135,** 308 (1972).
13. I. V. PETROVA, L. N. KAPLUNNIK, N. S. BORTNIKOV, E. A. POBEDIMSKAYA, AND N. V. BELOV, *Sov. Phys. Dokl. Engl. Transl.* **23,** 448 (1978).
14. N. WANG, *Neues Jahrb. Mineral. Monatsh.* 501 (1977).
15. E. MAKOVICKY, *Fortschr. Mineral.* **59,** 137 (1981).
16. A. D. WADSLEY, *Adv. Chem. Ser.* **39,** 23 (1963).
17. B. G. HYDE, S. ANDERSSON, M. BAKKER, C. M. PLUG, AND M. O'KEEFFE, *Prog. Solid State Chem.* **12,** 273 (1979).
18. D. MOOTZ AND H. PUHL, *Acta Crystallogr.* **23,** 471 (1967).
19. J. C. JUMAS, J. OLIVIER-FOURCADE, E. PHILIPPOT, AND M. MAURIN, *Rev. Chim. Miner.* **16,** 48 (1979).
20. I. V. PETROVA, A. I. KUZNETSOV, E. L. BELOKONEVA, M. A. SIMONOV, E. A. POBEDIMSKAYA, AND N. V. BELOV, *Sov. Phys. Dokl. Engl. Transl.* **23,** 630 (1978).
21. Y. OKA, A. KIKUCHI, T. MORI, AND E. SAWAGUCHI, *J. Phys. Soc. Japan* **21,** 405 (1966).